



<https://pubsonline.informs.org/journal/ijoc>

INFORMS JOURNAL ON COMPUTING

Vol. 00, No. 0, XXXXX 0000, pp. 000–000

Submitted to *INFORMS Journal on Computing*

ISSN 0899-1499, EISSN 1526-5528

Federated Online Learning for Heterogeneous Multisource Streaming Data

Jingmao Li*

Department of Biostatistics, Yale School of Public Health jingmao.li@yale.edu

Yuanxing Chen*

Yau Mathematical Sciences Center, Tsinghua University, chenyuanxing@tsinghua.edu.cn

Shuangge Ma

Department of Biostatistics, Yale School of Public Health shuangge.ma@yale.edu

Kuangnan Fang[†]

Department of Statistics and Data Science, School of Economics, Xiamen University xmufkn@xmu.edu.cn

Authors are encouraged to submit new papers to INFORMS journals by means of a style file template, which includes the journal title. However, use of a template does not certify that the paper has been accepted for publication in the named journal. INFORMS journal templates are for the exclusive purpose of submitting to an INFORMS journal and are not intended to be a true representation of the article's final published form. Use of this template to distribute papers in print or online or to submit papers to another non-INFORMS publication is prohibited.

Abstract. Federated learning has emerged as an essential paradigm for distributed multi-source data analysis under privacy concerns. Most existing federated learning methods focus on the “static” datasets. However, in many real-world applications, data arrive continuously over time, forming streaming datasets. This introduces additional challenges for data storage and algorithm design, particularly under high-dimensional settings. In this paper, we propose a federated online learning (FOL) method for distributed multi-source streaming data analysis. To account for heterogeneity, a personalized model is constructed for each data source, and a novel “subgroup” assumption is employed to capture potential similarities, thereby enhancing model performance. We adopt the penalized renewable estimation method and the efficient proximal gradient descent for model training. The proposed method aligns with both federated and online learning frameworks: raw data are not exchanged among sources, ensuring data privacy, and only summary statistics of previous data batches are required for model updates, significantly reducing storage demands. Theoretically, we establish the consistency properties for model estimation, variable selection, and subgroup structure recovery, demonstrating optimal statistical efficiency. Simulations illustrate the effectiveness of the proposed method. Furthermore, when applied to the financial lending data and the web log data, the proposed method also exhibits advantageous prediction performance. Results of the analysis also provide some practical insights.

Funding: This work was supported by the National Natural Science Foundation of China [Grants 72071169, 72233002], National Social Science Foundation of China [Grant 21&ZD146], Fundamental Research Funds for the Central Universities [Grant 20720231060], and the Shuimu Tsinghua Scholar Program of Tsinghua University.

Key words: Federated learning; online learning; streaming data; heterogeneity; high-dimensional.

* Joint first author.

† Correspondence author

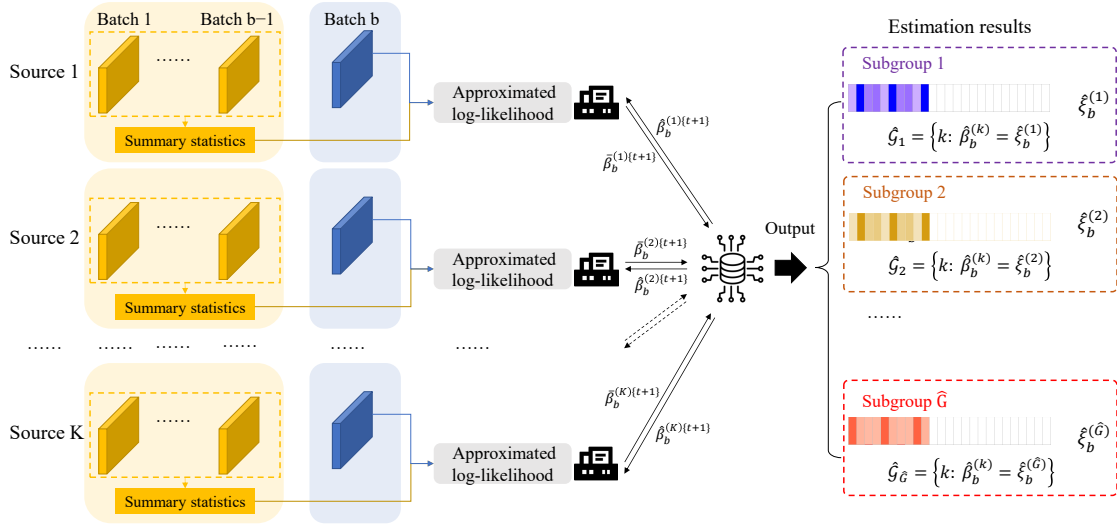
1. Introduction

Federated learning (FL) (McMahan et al. 2017) is a decentralized machine learning framework for analyzing distributed multisource data. In FL, individual data sources (clients) retain their local datasets, and privacy-preserving algorithms are used to collaboratively train models without sharing raw data. Based on assumptions about data distributions and model structures, FL methods can be broadly categorized into homogeneous and heterogeneous approaches. Homogeneous FL assumes a shared global model across all sources and aggregates all local information for model training. In contrast, heterogeneous FL allows for personalized models to accommodate source-specific heterogeneity. In this study, we focus on heterogeneous FL, which is often better suited to real-world applications. Substantial efforts have been made in FL; we refer to the comprehensive reviews for more details (Wen et al. 2023, Pei et al. 2024).

Despite the tremendous progress, most of the existing FL methods primarily focus on “static” data analysis. For this, data sources is capable to gather all the samples at once. However, advancements in data collection techniques have led to the emergence of multisource “streaming data”, as illustrated in left half of Figure 1. Here, data is collected from multiple sources, and each source can continuously receive new data batches (new samples) over time, significantly different from the “static” datasets. Our study is motivated by data from a national online financial lending platform in China. This platform collects daily updated business data from various provinces (data sources) to analyze user behavior in real-time. Another example is the continuously generated web log data across multiple websites, essential for cyberattack detection. Additional potential applications include fraud detection, the Internet of Things (IoT), healthcare, and e-Commerce (Gomes et al. 2019).

Multisource streaming data presents unique challenges compared to other data types. First, real-time data collection leads to high velocity and volume, requiring efficient analysis methods that avoid excessive storage and computational costs. Several online learning methods have been developed to analyze streaming data (Toulis and Airoldi 2017, Luo and

Figure 1 Diagram of distributed multisource streaming data and flowchart of the proposed federated online learning method.



Song 2020). These methods can train and update models without accessing data from previous batches, thereby substantially reducing storage and computation demands. However, most existing approaches focus primarily on single-source data, leaving methodological and theoretical development for multisource scenarios largely unexplored. Second, as a common challenge in multisource data analysis and heterogeneous federated learning (FL), data sources often exhibit both shared and source-specific structures. Therefore, it is crucial to develop methods that can effectively balance homogeneity and heterogeneity across sources.

Motivated by the above investigations, we propose a federated online learning (FOL) estimator for analyzing high-dimensional multi-source streaming data. We consider high-dimensional settings in which only a small subset of covariates is associated with the response, necessitating variable selection. To model heterogeneous multi-source data, we assume the existence of a latent subgroup structure across sources, where sources within the same subgroup share a common subgroup-specific model. This structure facilitates the modeling of both homogeneity and heterogeneity among sources, thereby enhancing

overall performance. To estimate the model, we develop an efficient algorithm based on the renewable estimation framework (Luo and Song 2020) and proximal gradient descent algorithm (Beck and Teboulle 2009). The proposed method updates the model using current data and historical summary statistics, and it does not require transmission of raw data across sources. Theoretically, we establish consistency in model estimation, variable selection, and subgroup structure recovery, achieving the same convergence rate as the “oracle” estimator and demonstrating optimal statistical efficiency. In summary, compared to existing studies, we propose a novel federated learning method for analyzing multisource streaming data, a setting that has received limited attention. Furthermore, our theoretical developments offer broader insights into the fields of federated and online learning, particularly in high-dimensional settings.

2. Literature Review

2.1. Federated Learning and multisource data analysis

Multi-source data analysis has gained considerable attention in diverse fields, including electronic health records (EHR) modeling and customer transaction records modeling (Qiu et al. 2024). Considering the privacy, FL learning (Yan et al. 2024, Qi et al. 2025) has emerged as an essential paradigm for this problem. FedAvg (McMahan et al. 2017) is the most basic FL method, which trains a global model by averaging locally updated models from multiple sources after multiple rounds of iterations. Although direct, FedAvg adopts a global model for all sources, neglecting the differences among sources. In contrast, heterogeneous or personalized FL methods aim to consider model heterogeneity under FL framework. They leverage shared information across sources to build similar personalized models for related sources, thereby enhancing the performance of customized models. For example, clustered FL (Chen et al. 2024) groups sources with similar data distributions or model parameters into clusters and trains separate models per cluster to better capture heterogeneity and improve overall performance. Knowledge distillation-based FL (Wang et al. 2024) enables collaboration and alignment among heterogeneous sources by having

them share soft predictions or representations. Other related methods include meta learning (Fallah et al. 2020) and regularization-based methods (T. Dinh et al. 2020). In addition to FL methods, other avenues of research have also investigated the multisource data analysis. For example, integrative analysis approaches (Huang et al. 2017, Maity et al. 2022) have attracted substantial interest, especially in high-dimensional scenarios. However, most of these methods do not explicitly address the challenges of streaming data analysis.

2.2. Online Learning

Traditional statistical methods typically fit models using raw data from both historical and newly arrived batches, which becomes impractical due to rapid data growth and storage constraints. In contrast, online learning enables model updates based on current individual-level data and summary statistics from previous batches, significantly reducing storage needs and the processing of extensive historical datasets. Among existing online learning methods, stochastic gradient descent (SGD) and its variants are well-regarded for their simplicity and effectiveness (Toulis and Airoldi 2017). Despite its computational convenience, reliance on first-order gradient information may limit efficiency and statistical inference (Ma et al. 2022). Recently, Luo and Song (2020) introduced a renewable estimation method based on second-order Taylor's expansion, which has been extended to high-dimensional analysis (Luo et al. 2023), quantile regression (Xie et al. 2024), and others.

A few recent studies have also focused on multisource streaming data analysis with online updates for global or source-specific model parameters. For example, Hector et al. (2023) proposed the Parallel-and-Stream Accelerator (PASA), which uses a divide-and-combine method for distributed online learning. However, its neglect of heterogeneity and high-dimensionality limits real-world applicability. Similarly, Luo and Li (2022) analyzes distributed streaming data using linear mixed-effects models to account for site-specific random effects, but this method is limited to linear models and panel data, and struggles with

high-dimensionality. Moreover, site-specific effects can introduce many redundant parameters, negatively impacting the estimation and prediction performance. Overall, existing methods are still insufficient in modeling high-dimensional multisource data.

3. Methodology

3.1. Data and Model

In the context of distributed multi-source streaming data, we assume the existence of K distinct sources, each continuously receiving b batches of data. Denote the observations collected in the u -th batch from the K distinct sources as $\mathcal{D}_u^{(k)} = \{y_{u,i}^{(k)}, \mathbf{x}_{u,i}^{(k)}\}_{i=1}^{n_{u,k}}$. Here, we denote $n_{u,k}$ as the sample size, $y_{u,i}^{(k)} \in \mathbb{R}$ as the response variable, and $\mathbf{x}_{u,i}^{(k)} \in \mathbb{R}^p$ as the p -dimensional covariate. For simplicity, we also denote $\tilde{\mathcal{D}}_b^{(k)} = \{\mathcal{D}_1^{(k)}, \dots, \mathcal{D}_b^{(k)}\}$ as the cumulative data for the k -th source up to batch b . We assume that $\mathcal{D}_u^{(k)}$ are independent and identically distributed across b batches and K sources. Define $N_{b,k} = \sum_{u=1}^b n_{u,k}$ as the cumulative sample size for the source k up to the b batches, and $N_b = \sum_{k=1}^K N_{b,k}$ as the total sample size for all K sources. For the k -th source, we assume that the conditional distribution of $y_{u,i}^{(k)}$ given $\mathbf{x}_{u,i}^{(k)}$ belongs to the canonical exponential family, of which the density function depends on the source-specific parameters $\boldsymbol{\beta}^{(k)} = (\beta_1^{(k)}, \dots, \beta_p^{(k)})^\top$ and is given by:

$$f(y_{u,i}^{(k)} | \mathbf{x}_{u,i}^{(k)}; \boldsymbol{\beta}^{(k)}) = c(y_{u,i}^{(k)}; \phi^{(k)}) \exp \left[y_{u,i}^{(k)} \mathbf{x}_{u,i}^{(k)\top} \boldsymbol{\beta}^{(k)} - d(\mathbf{x}_{u,i}^{(k)\top} \boldsymbol{\beta}^{(k)}) \right], \quad k \in [K], u \in [b], \quad (1)$$

where $d(\cdot)$ is the unit deviance function of the exponential family, $\phi^{(k)}$ is the dispersion parameter, and $c(\cdot)$ is the normalization term. For any integer b , we denote $[b] = \{1, \dots, b\}$.

Given the observed data, the model parameters in (1) can be naively estimated by minimizing the negative likelihood:

$$\hat{\boldsymbol{\beta}}_{b,\text{naive}}^{(k)} = \arg \min_{\boldsymbol{\beta}^{(k)}} \left\{ \mathcal{L}(\boldsymbol{\beta}^{(k)}; \tilde{\mathcal{D}}_b^{(k)}) = \sum_{u=1}^b \sum_{i=1}^{n_{u,k}} \left[y_{u,i}^{(k)} \mathbf{x}_{u,i}^{(k)\top} \boldsymbol{\beta}^{(k)} - d(\mathbf{x}_{u,i}^{(k)\top} \boldsymbol{\beta}^{(k)}) \right] \right\}, \quad k \in [K]. \quad (2)$$

However, this naive estimator has several limitations. First, optimizing (2) requires access to all raw data up to the b -th batch, which, given the high velocity and volume of streaming data, imposes significant storage and computational burdens. Second, the estimator in (2) treats each source independently, estimating model coefficients separately and thereby ignoring potential similarities and inter-source connections. In practice, however, sources often share some homogeneous information, which can be leveraged to improve model performance – particularly in high-dimensional settings (Huang et al. 2017).

To enhance estimation, we propose a novel Federated Online Learning (FOL) method for analyzing multi-source streaming data. Our aim is to develop a unified framework that accommodates both homogeneity and heterogeneity across data sources while adhering to federated and online learning paradigms. Specifically, following Luo and Song (2020), we first develop a strategy to approximate the log-likelihood of previous batches ($u \in [b-1]$) for source k ($k \in [K]$) using summary statistics. We first consider the case where $b = 2$, in which $\mathcal{D}_2^{(k)}$ arrives after $\mathcal{D}_1^{(k)}$ for all $k \in [K]$. To avoid using individual-level data from $\mathcal{D}_1^{(k)}$, we can adopt following least-square approximation:

$$\begin{aligned} \mathcal{L}(\boldsymbol{\beta}^{(k)}; \tilde{\mathcal{D}}_2^{(k)}) &= \mathcal{L}(\boldsymbol{\beta}^{(k)}; \mathcal{D}_1^{(k)}) + \mathcal{L}(\boldsymbol{\beta}^{(k)}; \mathcal{D}_2^{(k)}) \\ &= \mathcal{L}(\hat{\boldsymbol{\beta}}_1^{(k)}; \mathcal{D}_1^{(k)}) + \mathbf{U}(\hat{\boldsymbol{\beta}}_1^{(k)}; \mathcal{D}_1^{(k)})^\top (\boldsymbol{\beta}^{(k)} - \hat{\boldsymbol{\beta}}_1^{(k)}) \\ &\quad + \frac{1}{2} (\boldsymbol{\beta}^{(k)} - \hat{\boldsymbol{\beta}}_1^{(k)})^\top \mathbf{J}(\hat{\boldsymbol{\beta}}_1^{(k)}; \mathcal{D}_1^{(k)}) (\boldsymbol{\beta}^{(k)} - \hat{\boldsymbol{\beta}}_1^{(k)}) \\ &\quad + \mathcal{L}(\boldsymbol{\beta}^{(k)}; \mathcal{D}_2^{(k)}) + n_1^{(k)} O_p \left(\left\| \hat{\boldsymbol{\beta}}_1^{(k)} - \boldsymbol{\beta}^{(k)} \right\|_2 \right), \end{aligned} \quad (3)$$

where $\hat{\boldsymbol{\beta}}_1^{(k)}$ is the initial estimator from the first batch, while $\mathbf{U}(\boldsymbol{\beta}^{(k)}; \mathcal{D}_u^{(k)}) = \partial \mathcal{L}(\boldsymbol{\beta}^{(k)}; \mathcal{D}_u^{(k)}) / \partial \boldsymbol{\beta}^{(k)}$ and $\mathbf{J}(\boldsymbol{\beta}^{(k)}; \mathcal{D}_u^{(k)}) = \partial^2 \mathcal{L}(\boldsymbol{\beta}^{(k)}; \mathcal{D}_u^{(k)}) / \partial \boldsymbol{\beta}^{(k)} \partial \boldsymbol{\beta}^{(k)\top}$ represent the gradient vector and Hessian matrix, respectively. The initial estimator $\hat{\boldsymbol{\beta}}_1^{(k)}$ ensures $\mathbf{U}(\hat{\boldsymbol{\beta}}_1^{(k)}; \mathcal{D}_1^{(k)}) \approx \mathbf{0}$, which allows us to asymptotically ignore the error term. Consequently, the log-likelihood function $\mathcal{L}(\boldsymbol{\beta}^{(k)}; \tilde{\mathcal{D}}_2^{(k)})$ can be approximated as follows,

$$\hat{\mathcal{L}}_2^{(k)}(\boldsymbol{\beta}^{(k)}) := \frac{1}{2} (\boldsymbol{\beta}^{(k)} - \hat{\boldsymbol{\beta}}_1^{(k)})^\top \mathbf{J}(\hat{\boldsymbol{\beta}}_1^{(k)}; \mathcal{D}_1^{(k)}) (\boldsymbol{\beta}^{(k)} - \hat{\boldsymbol{\beta}}_1^{(k)}) + \mathcal{L}(\boldsymbol{\beta}^{(k)}; \mathcal{D}_2^{(k)}) + C, \quad (4)$$

where C denotes some irrelevant terms.

Now we generalize this approximation technique to the case where $b \geq 2$. After removing the irrelevant constant, the approximated log-likelihood function $\widehat{\mathcal{L}}_b^{(k)}(\boldsymbol{\beta}^{(k)})$ can be obtained as follows,

$$\widehat{\mathcal{L}}_b^{(k)}(\boldsymbol{\beta}^{(k)}) := \frac{1}{2}(\boldsymbol{\beta}^{(k)} - \widehat{\boldsymbol{\beta}}_{b-1}^{(k)})^\top \widehat{\mathbf{J}}_{b-1}^{(k)} (\boldsymbol{\beta}^{(k)} - \widehat{\boldsymbol{\beta}}_{b-1}^{(k)}) + \mathcal{L}(\boldsymbol{\beta}^{(k)}; \mathcal{D}_b^{(k)}), \quad (5)$$

where $\widehat{\boldsymbol{\beta}}_u^{(k)}$ ($k \in [K]$, $u \in [b]$) denotes the estimate from the u -th batch. For $b \geq 2$, we define the matrix $\widehat{\mathbf{J}}_{b-1}^{(k)} = \sum_{u=1}^{b-1} \mathbf{J}(\widehat{\boldsymbol{\beta}}_u^{(k)}; \mathcal{D}_u^{(k)})$, with $\widehat{\mathbf{J}}_0^{(k)} = \mathbf{0}_{p \times p}$ for consistency.

Meanwhile, to promote and utilize the potential similarity across different sources, we adopt a novel “subgroup” assumption among sources for analyzing multisource data. It hypothesis that there exists a subgroup partition $\mathcal{G} = \{\mathcal{G}^{(1)}, \dots, \mathcal{G}^{(G)}\}$ such that K sources can be categorized into G non-overlapping subgroups, where $G \geq 2$, $\mathcal{G}^{(g)} \subseteq [K]$, and $\cup_{g=1}^G \mathcal{G}^{(g)} = [K]$, and the sources within each subgroup share common parameters. Therefore, by accurately identifying the subgroup structure, we can facilitate the information sharing within the subgroup, thereby promoting the model estimation.

Therefore, given the approximated log-likelihood function (5), our FOL estimator $\widehat{\mathbf{B}}_b$ is obtained by minimizing the following objective function:

$$Q_b^{\text{on}}(\mathbf{B}) = -\frac{1}{N_b} \sum_{k=1}^K \widehat{\mathcal{L}}_b^{(k)}(\boldsymbol{\beta}^{(k)}) + \sum_{k=1}^K \sum_{j=1}^p \rho_a(|\beta_j^{(k)}|, \lambda_{1,b}) + \sum_{k_1 < k_2} \rho_a(\|\boldsymbol{\beta}^{(k_1)} - \boldsymbol{\beta}^{(k_2)}\|_2, \lambda_{2,b}). \quad (6)$$

where $\mathbf{B} = (\boldsymbol{\beta}^{(1)}, \dots, \boldsymbol{\beta}^{(K)})$ is a $p \times K$ coefficient matrix, $\|\cdot\|_2$ denotes the L_2 -norm, and $\rho_a(x, \lambda)$ is the penalty function characterized by tuning parameters λ and a . In this paper, we adopt the minimax concave penalty (MCP) (Zhang 2010), defined as $\rho_a(x, \lambda) = \int_0^{|x|} (\lambda - t/a)_+ dt$ for $x \in \mathbb{R}$. The second term of $Q_b^{\text{on}}(\mathbf{B})$ in (6) serves as a sparsity penalty to select important variables, while the third term penalizes the pairwise differences between $\boldsymbol{\beta}^{(k_1)}$ and $\boldsymbol{\beta}^{(k_2)}$ (for $k_1 < k_2$), therefore promoting the identification of subgroup structure. Specifically, if $\|\boldsymbol{\beta}^{(k_1)} - \boldsymbol{\beta}^{(k_2)}\|_2$ approaches 0, then sources k_1 and k_2 are regarded to

belong to the same subgroup. This fusion penalty has shown its unique advantages and is commonly employed for clustering or identification of the coefficient structure (Ma and Huang 2017).

It is noted that for the objective function $Q_b^{\text{on}}(\mathbf{B})$ in (6), we do not need to access historical data batches. Instead, we can sequentially use and update the summary statistics $\{\widehat{\mathbf{J}}_{b-1}^{(k)}, \widehat{\boldsymbol{\beta}}_{b-1}^{(k)}\}_{k \in [K]}$. Meanwhile, as discussed in subsequent sections, we optimize the objective function using federated learning, which does not require the transmission of raw data across sources. The right panel of Figure 1 presents the flowchart of the proposed FOL method. Overall, the method automatically identifies subgroup structures across data sources, effectively capturing both homogeneity and heterogeneity, thereby improving estimation and prediction performance.

3.2. Computational Algorithm

We implement the proximal gradient algorithm (Beck and Teboulle 2009) to solve (6). This algorithm is a variant of traditional gradient descent, capable of optimizing non-differentiable objective functions. The algorithm iterates a local calculation step under each data source and a master aggregation step under a central server, which accommodates the federated learning paradigm. Specifically, with estimated coefficients $\widehat{\mathbf{B}}_b^{\{t\}} = (\widehat{\boldsymbol{\beta}}_b^{(1)\{t\}}, \dots, \widehat{\boldsymbol{\beta}}_b^{(K)\{t\}})$ in the t -th iteration, we process the two steps as follows:

- **Step I. local calculation.** For the k -th source, we update the parameter based on gradient descent:

$$\widehat{\boldsymbol{\beta}}_b^{(k)\{t+1\}} = \widehat{\boldsymbol{\beta}}_b^{(k)\{t\}} - \omega \mathbf{g}_b^{(k)\{t+1\}}, \quad (7)$$

where ω is the learning rate, and $\mathbf{g}_b^{(k)\{t+1\}}$ denotes the gradient of the loss function, calculated by

$$\mathbf{g}_b^{(k)\{t+1\}} = -\frac{1}{N_b} \frac{\partial \widehat{\mathcal{L}}_b^{(k)}(\widehat{\boldsymbol{\beta}}_b^{(k)\{t\}})}{\partial \widehat{\boldsymbol{\beta}}_b^{(k)\{t\}}} = -\frac{1}{N_b} \left[\mathbf{U}(\widehat{\boldsymbol{\beta}}_b^{(k)\{t+1\}}; \mathcal{D}_b^{(k)}) + \widehat{\mathbf{J}}_{b-1}^{(k)}(\widehat{\boldsymbol{\beta}}_b^{(k)\{t+1\}} - \widehat{\boldsymbol{\beta}}_{b-1}^{(k)}) \right]. \quad (8)$$

After the calculation, we transmit the updated model parameter $\widehat{\boldsymbol{\beta}}_b^{(k)\{t+1\}}$ to the master server.

- **Step II. master aggregation.** The master server aggregates all the updated model parameters $\bar{\mathbf{B}}_b^{\{t+1\}} = (\bar{\beta}_b^{(1)\{t+1\}}, \dots, \bar{\beta}_b^{(K)\{t+1\}})$, and use the proximal operator to get the output for the $(t+1)$ -th iteration:

$$\hat{\mathbf{B}}_b^{\{t+1\}} = \mathcal{P}_a \left(\bar{\mathbf{B}}_b^{\{t+1\}}; \lambda_{1,b}, \lambda_{2,b} \right), \quad (9)$$

where the function $\mathcal{P}_a(\bar{\mathbf{B}}_b^{\{t+1\}}; \lambda_{1,b}, \lambda_{2,b})$ denotes the proximal operator associated with the penalty terms in (6), which is defined as:

$$\mathcal{P}_a(\bar{\mathbf{B}}_b^{\{t+1\}}; \lambda_{1,b}, \lambda_{2,b}) = \arg \min_{\mathbf{B}} \frac{1}{2} \left\| \mathbf{B} - \bar{\mathbf{B}}_b^{\{t+1\}} \right\|_F^2 + \sum_{k=1}^K \sum_{j=1}^p \rho_a \left(\left| \beta_j^{(k)} \right|, \lambda_{1,b} \right) + \sum_{k_1 < k_2} \rho_a \left(\left\| \boldsymbol{\beta}^{(k_1)} - \boldsymbol{\beta}^{(k_2)} \right\|_2, \lambda_{2,b} \right), \quad (10)$$

where $\|\cdot\|_F$ denotes the Frobenius norm. We use the alternating direction method of multipliers (ADMM) (Boyd et al. 2011) to solve the optimization problem (10). The detailed calculation procedures are presented in Section S1.1 of the supplementary material.

Overall, we optimize (6) by repeating Steps I-II until convergence. The convergence properties for proximal gradient descent have been widely investigated in the literature (Li et al. 2017), and in most of our numerical studies, the convergence can be achieved within 50 iterations. The detailed procedures are outlined in Algorithm S1 of the supplementary material. The objective function includes three tuning parameters: $\lambda_{1,b}$, $\lambda_{2,b}$, and a . In our numerical study, we set $a = 3$ (Zhang 2010) and perform a grid search with modified Bayesian information criteria (mBIC; Ma and Huang 2017) to select $\lambda_{1,b}$ and $\lambda_{2,b}$. Further details on mBIC calculations can be found in Section S1.2 of the supplementary material.

4. Theoretical properties

4.1. Notations and Definitions

We introduce the following essential definitions. For the u -th batch from source k , let $\mathbf{X}_u^{(k)} = (\mathbf{x}_{u,1}^{(k)}, \dots, \mathbf{x}_{u,n_{u,k}}^{(k)})^\top$ be the design matrix and $\mathbf{Y}_u^{(k)} = (y_{u,1}^{(k)}, \dots, y_{u,n_{u,k}}^{(k)})^\top$ be the response vector. We define $\boldsymbol{\varphi}_u^{(k)} = \mathbf{X}_u^{(k)} \boldsymbol{\beta}^{(k)}$ and let $\mathbf{d}(\boldsymbol{\varphi}_u^{(k)}) = [d(\varphi_{u,1}^{(k)}), \dots, d(\varphi_{u,n_{u,k}}^{(k)})]^\top$ be a vector function of $\boldsymbol{\varphi}_u^{(k)}$. For simplicity, let $\boldsymbol{\mu}(\boldsymbol{\varphi}_u^{(k)}) = \mathbf{d}'(\boldsymbol{\varphi}_u^{(k)})$ and $\boldsymbol{\Sigma}(\boldsymbol{\varphi}_u^{(k)}) = \text{diag}\{\mathbf{d}''(\boldsymbol{\varphi}_u^{(k)})\}$. Let $|\mathcal{G}_{\min}| = \min_{g \in [G]} |\mathcal{G}^{(g)}|$ denote the minimal subgroup size. Define

$n_u^{(g)} = \sum_{k \in \mathcal{G}^{(g)}} n_{u,k}$, $u \in [b]$ as the sample size of aggregated sources in subgroup g for the u -th batch, and $N_b^{(g)} = \sum_{k \in \mathcal{G}^{(g)}} N_{b,k} = \sum_{u=1}^b n_u^{(g)}$ as the cumulative sample size up to batch b . We denote $\bar{N}_b = \min_{g \in [G]} N_b^{(g)}$. Let $\mathbf{B}^* = (\boldsymbol{\beta}^{*(1)}, \dots, \boldsymbol{\beta}^{*(K)})$ denote the true coefficient matrix corresponding to \mathbf{B} . Define $\mathcal{B}_k = \{j \in [p] : \boldsymbol{\beta}_j^{*(k)} \neq 0\}$ as the support of $\boldsymbol{\beta}^{*(k)}$, with \mathcal{B}_k^c denoting its complement. Accordingly, let $\boldsymbol{\Xi} = (\boldsymbol{\xi}^{(1)}, \dots, \boldsymbol{\xi}^{(G)})$ be the distinct coefficient matrix, where $\boldsymbol{\xi}^{(g)} = \boldsymbol{\beta}^{(k)}$ for any $k \in \mathcal{G}^{(g)}$, and $\boldsymbol{\Xi}^* = (\boldsymbol{\xi}^{*(1)}, \dots, \boldsymbol{\xi}^{*(G)})$ be the corresponding true coefficient matrix. We define $\mathcal{A}_g = \mathcal{B}_k$ for any $k \in \mathcal{G}^{(g)}$ as the index set for significant variables in g -th subgroup, $s_g = |\mathcal{A}_g|$ as the corresponding cardinality. Denote $s = \max_g s_g$.

Consider the following two subspaces of $\mathbb{R}^{p \times K}$:

$$\begin{aligned} \mathcal{M}_{\mathcal{G}} &= \left\{ \mathbf{B} \in \mathbb{R}^{p \times K} : \boldsymbol{\beta}^{(k_1)} = \boldsymbol{\beta}^{(k_2)}, \text{ for any } k_1, k_2 \in \mathcal{G}^{(g)}, g \in [G] \right\}, \\ \mathcal{M}_{\mathcal{B}} &= \left\{ \mathbf{B} \in \mathbb{R}^{p \times K} : \boldsymbol{\beta}_{\mathcal{B}_k^c}^{(k)} = \mathbf{0}_{p-s_g}, \text{ for any } k \in \mathcal{G}^{(g)}, g \in [G] \right\}. \end{aligned} \quad (11)$$

When the true subgroup structure $\mathcal{G} = \{\mathcal{G}^{(1)}, \dots, \mathcal{G}^{(G)}\}$ and the sparsity structure $\{\mathcal{A}_g : g \in [G]\}$ are known, the “subgroup-sparsity-oracle” estimator for \mathbf{B} (up to batch b) is defined as

$$\widehat{\mathbf{B}}_b^{or} = \arg \min_{\mathbf{B} \in \mathcal{M}_{\mathcal{G}} \cap \mathcal{M}_{\mathcal{B}}} \left\{ \widehat{\mathcal{L}}_b(\mathbf{B}) = -\frac{1}{N_b} \sum_{k=1}^K \widehat{\mathcal{L}}_b^{(k)}(\boldsymbol{\beta}^{(k)}) \right\}. \quad (12)$$

It can be shown that, minimizing $\widehat{\mathcal{L}}_b(\mathbf{B})$ under the feasible set $\mathcal{M}_{\mathcal{G}} \cap \mathcal{M}_{\mathcal{B}}$ is equivalent to the constrained minimization of $\boldsymbol{\Xi}$ in that

$$\widehat{\boldsymbol{\Xi}}_b^{or} = \arg \min_{\boldsymbol{\Xi} \in \mathcal{M}_{\mathcal{A}}^{or}} \left\{ \widehat{\mathcal{L}}_b^{or}(\boldsymbol{\Xi}) = -N_b^{-1} \sum_{g \in [G]} \sum_{k \in \mathcal{G}^{(g)}} \widehat{\mathcal{L}}_b^{(k)}(\boldsymbol{\xi}^{(g)}) \right\}, \quad (13)$$

where $\mathcal{M}_{\mathcal{A}}^{or} = \left\{ \boldsymbol{\Xi} \in \mathbb{R}^{p \times G} : \boldsymbol{\xi}_{\mathcal{A}_g^c}^{(g)} = \mathbf{0}_{p-s_g}, g \in [G] \right\}$.

4.2. Asymptotic properties

In our theory, we consider a scenario where the sample size for each batch, denoted as $n_{u,k}$, is divergent. For simplicity, we assume that $n_{u,k} \asymp n_{u,*}$ for $u \in [b]$ and $k \in [K]$, implying $N_{u,k} \asymp N_{u,*}$. Furthermore, the number of variables (p), important variables (s),

and sources (K) can all go to infinity. To establish the asymptotic properties, we outline some regularity conditions in the following.

Condition 1 *Data $\{(\mathbf{x}_{u,i}^{(k)}, y_{u,i}^{(k)}) : k \in [K], u \in [b], i \in [n_{u,k}]\}\$ are independent and identically distributed. Moreover, there exists a constant $C_x > 0$ such that*

$$\begin{aligned} \max_{k \in [K], u \in [b]} \|\mathbf{X}_u^{(k)}\|_{\max} &\leq C_x, \\ \sigma_{\max} \left[\mathbf{X}_{u,\mathcal{A}_g}^{(k)\top} \mathbf{X}_{u,\mathcal{A}_g}^{(k)} \right] &\leq C_x n_{u,k}, \quad k \in \mathcal{G}^{(g)}, g \in [G], \end{aligned} \quad (14)$$

where $\|\cdot\|_{\max}$ and $\sigma_{\max}(\cdot)$ denote the maximal absolute value and the maximum eigenvalue of the matrix.

Condition 2 *Define the minimal signal level $d_1 = \min_{g \in [G], j \in \mathcal{A}_g, k \in \mathcal{G}^{(g)}} |\beta_j^{*(k)}|$ and the minimal distance between different subgroups $d_2 = \min_{g_1 \neq g_2 \in [G], k_1 \in \mathcal{G}^{(g_1)}, k_2 \in \mathcal{G}^{(g_2)}} \|\boldsymbol{\beta}^{*(k_1)} - \boldsymbol{\beta}^{*(k_2)}\|_2$. For $u \in [b]$, assume $d_1 > 2a\lambda_{1,u}$, $d_2 > 2a\lambda_{2,u}$, and $\lambda_{1,u} \gg \sqrt{[\log(pK) + s]/\bar{N}_u}$, $\lambda_{2,u} \gg \sqrt{s/\bar{N}_u}$.*

Condition 3 *For the g -th ($g \in [G]$) subgroup, define the neighborhood around the vector of true coefficients $\boldsymbol{\xi}_{\mathcal{A}_g}^{*(g)}$ as $\mathcal{N}_0^{(g)} = \{\boldsymbol{\xi}_{\mathcal{A}_g} \in \mathbb{R}^{s_g} : \|\boldsymbol{\xi}_{\mathcal{A}_g} - \boldsymbol{\xi}_{\mathcal{A}_g}^{*(g)}\|_{\infty} \leq d_1/2\}$. Then for each $k \in \mathcal{G}^{(g)}$ and batch $u = 1, \dots, b$, we assume that*

$$\min_{\alpha \in \mathcal{N}_0^{(g)}} \sigma_{\min} \left[\mathbf{X}_{u,\mathcal{A}_g}^{(k)\top} \boldsymbol{\Sigma} (\mathbf{X}_{u,\mathcal{A}_g}^{(k)} \boldsymbol{\alpha}) \mathbf{X}_{u,\mathcal{A}_g}^{(k)} \right] \geq c_1 n_{u,k}, \quad (15)$$

$$\max_{\alpha \in \mathcal{N}_0^{(g)}} \sigma_{\max} \left[\mathbf{X}_{u,\mathcal{A}_g}^{(k)\top} \boldsymbol{\Sigma} (\mathbf{X}_{u,\mathcal{A}_g}^{(k)} \boldsymbol{\alpha}) \mathbf{X}_{u,\mathcal{A}_g}^{(k)} \right] \leq C_1 n_{u,k}, \quad (16)$$

$$\max_{\alpha \in \mathcal{N}_0^{(g)}} \max_{j=1}^p \sigma_{\max} \left[\mathbf{X}_{u,\mathcal{A}_g}^{(k)\top} \text{diag} \left\{ |\mathbf{X}_{u,j}^{(k)\top}| \circ \mathbf{d}'''(\mathbf{X}_{u,\mathcal{A}_g}^{(k)} \boldsymbol{\alpha}) \right\} \mathbf{X}_{u,\mathcal{A}_g}^{(k)} \right] \leq C_2 n_{u,k}, \quad (17)$$

where c_1 , C_1 and C_2 are three positive constants, $\sigma_{\min}(\cdot)$ denotes the minimal eigenvalue of the matrix.

Condition 4 For each subgroup $g \in [G]$ and batch $u \in [b]$, it satisfies that for any $n_u^{(g)}$ -dimensional vector $\boldsymbol{\eta}$ and $\epsilon > 0$,

$$\Pr \left[\left| \boldsymbol{\eta}^\top \left\{ \widetilde{\mathbf{Y}}_u^{(g)} - \boldsymbol{\mu}(\widetilde{\mathbf{X}}_u^{(g)} \boldsymbol{\xi}^{*(g)}) \right\} \right| < \|\boldsymbol{\eta}\|_2 \epsilon \right] > 1 - 2 \exp \left[-\kappa \epsilon^2 \right], \quad (18)$$

where $\widetilde{\mathbf{X}}_u^{(g)} = (\mathbf{X}_u^{(k)\top}, k \in \mathcal{G}^{(g)})^\top$, $\widetilde{\mathbf{Y}}_u^{(g)} = (\mathbf{Y}_u^{(k)\top}, k \in \mathcal{G}^{(g)})^\top$, and $\kappa > 0$ is a constant.

Condition 5 For any g -th ($g \in [G]$) subgroup, we assume that

$$\left\| \mathbf{X}_{u, \mathcal{A}_g^c}^{(k)\top} \boldsymbol{\Sigma}(\mathbf{X}_u^{(k)} \boldsymbol{\beta}^{*(k)}) \mathbf{X}_{u, \mathcal{A}_g}^{(k)} \right\|_{2, \infty} \leq C_3 n_{u, k}, \quad k \in \mathcal{G}^{(g)}, u \in [b], \quad (19)$$

where C_3 is a positive constant. For matrix \mathbf{H} , $\|\mathbf{H}\|_{2, \infty} = \max_{\mathbf{x} \in \mathbb{R}^p, \|\mathbf{x}\|_2=1} \|\mathbf{H}\mathbf{x}\|_\infty$.

Condition 6 The penalty function $\rho_a(x, \lambda)$ is a symmetric function of x with $\rho_a(0, \lambda) = 0$. It is non-decreasing and concave in $[0, +\infty)$. Its first-order derivative $\rho'_a(x, \lambda)$ exists and is continuous for $x \in [0, \infty)$, $\rho'_a(0+, \lambda) = \lambda$. $\rho_a(x, \lambda)$ equals to a constant $C_{\lambda, a}$ for $|x| \geq a\lambda$, i.e., $\rho'_a(x, \lambda) = 0$ for $|x| \geq a\lambda$.

The detailed explanation for these conditions is summarized in the Supplementary Material Section S2. Based on the conditions, we can develop the following theoretical properties.

THEOREM 1. Consider the online estimate in the first batch ($b = 1$). Under Conditions 1 – 6, we have that

(1) The “subgroup-sparsity-oracle” common coefficient estimator defined in (13) satisfies:

$$\max_{g \in [G]} \left\| \widehat{\boldsymbol{\xi}}_{1, \mathcal{A}_g}^{or(g)} - \boldsymbol{\xi}_{\mathcal{A}_g}^{*(g)} \right\|_2 = O_p \left(\sqrt{s/\bar{N}_1} \right),$$

which implies that the “subgroup-sparsity-oracle” estimator defined in (12) also satisfies that $\max_{k \in [K]} \left\| \widehat{\boldsymbol{\beta}}_{1, \mathcal{B}_k}^{or(k)} - \boldsymbol{\beta}_{\mathcal{B}_k}^{*(k)} \right\|_2 = O_p \left(\sqrt{s/\bar{N}_1} \right)$.

(2) There exists a strictly local minimizer $\widehat{\mathbf{B}}_1$ of $Q_1^{on}(\mathbf{B})$ that $\Pr[\widehat{\mathbf{B}}_1 = \widehat{\mathbf{B}}_1^{or}] \rightarrow 1$.

Theorem 1 establishes the consistency of the estimated coefficients for the first batch ($b = 1$) based on the offline estimate. Result (1) shows the consistency of the “subgroup-sparsity-oracle” estimator for common subgroup coefficients $\widehat{\mathbf{B}}_1^{or}$, that is, $\max_{k \in [K]} \|\widehat{\beta}_{1, \mathcal{B}_k}^{or(k)} - \beta_{\mathcal{B}_k}^{*(k)}\|_2$ converges at a rate of $\sqrt{s/\bar{N}_1}$. Result (2) further indicates that $\widehat{\mathbf{B}}_1^{or}$ is a strictly local minimizer of $Q_1^{on}(\mathbf{B})$ in (6) with probability approaching 1. Together, these results imply that $\widehat{\mathbf{B}}_1$ is asymptotically equivalent to $\widehat{\mathbf{B}}_1^{or}$ and then inherits the same convergence rate. Consequently, since both variable selection and clustering rely on this structure, we conclude that $\Pr[\cap_{k=1}^K \{\widehat{\mathcal{B}}_k = \mathcal{B}_k\}] \rightarrow 1$ and $\Pr[\widehat{\mathcal{G}} = \mathcal{G}] \rightarrow 1$, indicating consistency in variable selection and clustering.

THEOREM 2. *Consider the online estimate in the b -th batch ($b \geq 2$). Under Conditions 1 – 6, we have that*

(1) *The “subgroup-sparsity-oracle” common coefficient estimator defined in (13) satisfies:*

$$\max_{g \in [G]} \|\widehat{\xi}_{b, \mathcal{A}_g}^{or(g)} - \xi_{\mathcal{A}_g}^{*(g)}\|_2 = O_p\left(\sqrt{s/\bar{N}_b}\right),$$

which directly implies the “subgroup-sparsity-oracle” estimator defined in (12) also satisfies that $\max_{k \in [K]} \|\widehat{\beta}_{b, \mathcal{B}_k}^{or(k)} - \beta_{\mathcal{B}_k}^{(k)}\|_2 = O_p\left(\sqrt{s/\bar{N}_b}\right)$.*

(2) *There exists a strictly local minimizer $\widehat{\mathbf{B}}_b$ of $Q_b^{on}(\mathbf{B})$ that $\Pr[\widehat{\mathbf{B}}_b = \widehat{\mathbf{B}}_b^{or}] \rightarrow 1$.*

Theorem 2 establishes the consistency of online estimates using results from Theorem 1 and an inductive approach. Similar to Theorem 1, the estimator $\widehat{\mathbf{B}}_b$ from the b -th batch converges at the rate: $\max_{k \in [K]} \|\widehat{\beta}_{b, \mathcal{B}_k}^{(k)} - \beta_{\mathcal{B}_k}^{*(k)}\|_2 = O_p\left(\sqrt{s/\bar{N}_b}\right)$, ensuring consistency in variable selection and clustering. Compared to $\widehat{\mathbf{B}}_1$ from the first batch, $\widehat{\mathbf{B}}_b$ converges faster due to the larger sample size \bar{N}_b , matching the convergence rate of the offline estimator. Therefore, Theorem 2 indicates that $\widehat{\mathbf{B}}_b$ is asymptotically equivalent to $\widetilde{\mathbf{B}}_b$, consistent with the online learning literature (Luo and Song 2020). However, the high-dimensional, multi-source data settings introduce unique theoretical challenges. Additionally, the consistency

in clustering shares similarities with integrative analysis and federated clustering literature. To the best of our knowledge, this property has not been explored in online learning. Thus, our investigation provides unique contributions to this field.

5. Simulation Studies

In this section, we conduct simulations to evaluate the finite sample performance of the proposed method. The data generation process is as follows: (a) We consider scenarios with $K \in \{8, 16, 32\}$ sources, with streaming data arriving in 10 batches. Each source starts with 100 subjects ($n_{1,k} = 100$ for $k \in [K]$), followed by $n_{u,k} \in \{40, 80\}$ subjects in subsequent batches ($u = 2, \dots, 10$). (b) The number of covariates is set at $p \in \{50, 100, 200\}$. The covariates are generated from a multivariate normal distribution with a mean of zero and an autoregressive covariance structure: $\mathbf{x}_{u,i}^{(k)} \sim N(\mathbf{0}_p, \Sigma_p)$, where $[\Sigma_p]_{i,j} = 0.5^{|i-j|}$. (c) The response variable $y_{u,i}^{(k)}$ is randomly drawn from the distribution $f(y| \mathbf{x}_{u,i}^{(k)}, \boldsymbol{\beta}^{(k)})$. We use logistic and linear regression analysis in our simulations.

We explore three examples to illustrate various subgroup structures among data sources. Specifically, Example 1 depicts a homogeneous scenario in which all sources share the same model. In contrast, Examples 2 and 3 present heterogeneous scenarios, with models for different sources grouped into 2 and 4 subgroups, respectively.

Example 1. In this homogeneous case, we have $\boldsymbol{\beta}^{*(k)} = \boldsymbol{\xi}^*$ for $k = 1, \dots, 8$. We randomly select two disjoint subsets of variables, C_1 and C_2 , each containing 4 variables. The coefficient vector $\boldsymbol{\xi}^*$ is defined as: $\boldsymbol{\xi}_{C_1}^* = 0.6\mathbf{1}_4$, $\boldsymbol{\xi}_{C_2}^* = -0.6\mathbf{1}_4$ and $\boldsymbol{\xi}_{C_1^c \cap C_2^c}^* = \mathbf{0}_{p-8}$.

Example 2. In this case, coefficients from different sources are divided into two subgroups: $\boldsymbol{\beta}^{*(k)} = \boldsymbol{\xi}^{*(1)}$ for $k = 1, \dots, 4$ and $\boldsymbol{\beta}^{*(k)} = \boldsymbol{\xi}^{*(2)}$ for $k = 5, \dots, 8$, with $\boldsymbol{\xi}^{*(1)} \neq \boldsymbol{\xi}^{*(2)}$. The index sets C_1 and C_2 are defined similarly to Example 1, with coefficient vectors given by: (i) $\boldsymbol{\xi}_{C_1}^{(1)*} = 0.6\mathbf{1}_4$, $\boldsymbol{\xi}_{C_2}^{(1)*} = -0.6\mathbf{1}_4$, $\boldsymbol{\xi}_{C_1^c \cap C_2^c}^{(1)*} = \mathbf{0}_{p-8}$; and (ii) $\boldsymbol{\xi}_{C_1}^{(2)*} = -0.6\mathbf{1}_4$, $\boldsymbol{\xi}_{C_2}^{(2)*} = 0.6\mathbf{1}_4$, $\boldsymbol{\xi}_{C_1^c \cap C_2^c}^{(2)*} = \mathbf{0}_{p-8}$.

Example 3. Here, coefficients from different sources are divided into four subgroups: $\boldsymbol{\beta}^{*(k)} = \boldsymbol{\xi}^{*(1)}$ for $k = 1, 2$, $\boldsymbol{\beta}^{*(k)} = \boldsymbol{\xi}^{*(2)}$ for $k = 3, 4$, $\boldsymbol{\beta}^{*(k)} = \boldsymbol{\xi}^{*(3)}$ for $k = 5, 6$, and $\boldsymbol{\beta}^{*(k)} = \boldsymbol{\xi}^{*(4)}$

for $k = 7, 8$, with $\boldsymbol{\xi}^{(1)*} \neq \boldsymbol{\xi}^{*(2)} \neq \boldsymbol{\xi}^{*(3)} \neq \boldsymbol{\xi}^{*(4)}$. The index sets C_1 and C_2 are defined as in Example 1, with the following coefficient vectors: (i) $\boldsymbol{\xi}_{C_1}^{(1)*} = 0.6\mathbf{1}_4$, $\boldsymbol{\xi}_{C_2}^{(1)*} = 0.6\mathbf{1}_4$, $\boldsymbol{\xi}_{C_1^c \cap C_2^c}^{(1)*} = \mathbf{0}_{p-8}$; (ii) $\boldsymbol{\xi}_{C_1}^{(2)*} = -0.6\mathbf{1}_4$, $\boldsymbol{\xi}_{C_2}^{(2)*} = 0.6\mathbf{1}_4$, $\boldsymbol{\xi}_{C_1^c \cap C_2^c}^{(2)*} = \mathbf{0}_{p-8}$; (iii) $\boldsymbol{\xi}_{C_1}^{(1)*} = 0.6\mathbf{1}_4$, $\boldsymbol{\xi}_{C_2}^{(1)*} = -0.6\mathbf{1}_4$, $\boldsymbol{\xi}_{C_1^c \cap C_2^c}^{(1)*} = \mathbf{0}_{p-8}$; and (iv) $\boldsymbol{\xi}_{C_1}^{(2)*} = -0.6\mathbf{1}_4$, $\boldsymbol{\xi}_{C_2}^{(2)*} = -0.6\mathbf{1}_4$, $\boldsymbol{\xi}_{C_1^c \cap C_2^c}^{(2)*} = \mathbf{0}_{p-8}$.

In addition to the proposed approach, we examine several relevant alternatives: (a) Oracle: This is an offline federated learning method, which assumes that we have simultaneous access to all data batches. The objective function for Oracle is similar to the proposed method, except that no approximation is adopted for the log-likelihood function. Although impractical for data streaming scenarios, Oracle serves as a benchmark for comparison. (b) Ind: This is the individualized online learning method. It updates the model in each source independently while ignoring potential connections between them. (c) Homo: This is the online divide-and-conquer method, which assumes homogeneity among sources. It first updates each data source, similar to Ind, and then aggregates the results to get a global estimation.

We evaluate these methods based on variable selection, estimation, prediction, and clustering. For variable selection, we use the average true positive rate (TPR) and false positive rate (FPR) across all sources. Estimation performance is assessed using the sum of squared errors $SSE = (1/K) \sum_{k=1}^K \|\widehat{\boldsymbol{\beta}}_u^{(k)} - \boldsymbol{\beta}^{*(k)}\|_2^2$. For prediction, we generate 2000 independent test samples for each source and evaluate performance with mean squared error (MSE) for linear regression and area under curve (AUC) for logistic regression. For clustering, we analyze the number of identified subgroups (\widehat{G}) and the adjusted rand index (ARI), which measures the agreement between the identified and true cluster structures, ranging from -1 to 1 (higher values indicate better agreement). Note that Ind and Homo cannot cluster data sources, so their clustering performance is not evaluated.

The simulation results from 100 replicates are reported in Table 1, together with additional tables and figures in Section S3 of the supplementary material. Observations are similar across settings. In the homogeneous example (Example 1), the proposed method

effectively identifies the underlying subgroup structure for data sources and improves performance in variable selection, estimation, and prediction. It outperforms the Ind method and demonstrates the advantages of our joint learning strategy. The proposed method slightly outperforms the Homo method and is comparable to the infeasible Oracle method, also indicating its effectiveness. Similar patterns can be observed in heterogeneous scenarios (Examples 2 and 3). Figures S1–S3 in the supplementary material show the trace plots of AUC (logistic regression) and MSE (linear regression), as well as the SSE for coefficient estimation across batches. Overall, the performance of Ind and the proposed method improves with more batches, and the proposed method generally outperforms Ind, underscoring the competitive performance of the proposed estimator.

6. Real Data Application

6.1. Analysis of financial platform data

We apply the proposed method to financial data from a peer-to-peer (P2P) lending platform to predict the success of credit-accredited bids. On this platform, users seeking funding post bids containing personal details (e.g., age, gender, marital status), bid specifics (e.g., total funds sought, borrowing period, interest rate), reasons for borrowing, and other relevant information. Investors use this data to determine whether and how much to invest. A bid is labeled as “successful” if it secures sufficient funding; otherwise, it is marked as “lost”. Predicting the success or failure of new bids based on user and bid information is crucial for the P2P platform, as it can highlight key factors influencing successful fundraising and offer valuable insights into the platform’s operations and growth.

The dataset contains credit-accredited bid information from $K = 13$ provinces (data sources) in China, collected over 13 days from September 7 to September 16, 2020, totaling 8,631 observations. Table S9 presents the sample sizes from various sources and batches. Sample sizes vary by source: Guangdong has the most observations, with 1,441 observations (48 to 79 per batch), while Jiangxi has the least at 489 (31 to 46 per batch). In contrast, the sample sizes are relatively balanced between different batches for each

Table 1 Simulation results for Example 2 with the logistic regression model, using $K = 8$ data sources. Each cell displays the mean (sd) based on 100 replicates.

p	$n_{u,k}$	Method	TPR	FPR	SSE	AUC	\widehat{G}	ARI
40	50	Oracle	1.00(0.00)	0.00(0.01)	0.036(0.012)	0.826(0.020)	2.0(0.0)	1.00(0.00)
		Ind	0.61(0.09)	0.01(0.01)	1.287(0.232)	0.761(0.035)	-	-
		Homo	0.99(0.03)	0.10(0.05)	2.976(0.041)	0.501(0.003)	-	-
		Proposed	0.95(0.06)	0.00(0.01)	0.227(0.189)	0.818(0.023)	2.0(0.2)	0.99(0.05)
80	100	Oracle	1.00(0.00)	0.00(0.00)	0.024(0.013)	0.828(0.012)	2.0(0.0)	1.00(0.00)
		Ind	0.71(0.07)	0.01(0.01)	0.968(0.203)	0.783(0.022)	-	-
		Homo	1.00(0.00)	0.06(0.04)	2.947(0.042)	0.499(0.004)	-	-
		Proposed	0.99(0.02)	0.00(0.00)	0.069(0.093)	0.826(0.014)	2.0(0.0)	1.00(0.00)
40	200	Oracle	1.00(0.00)	0.00(0.00)	0.036(0.011)	0.825(0.014)	2.0(0.0)	1.00(0.00)
		Ind	0.51(0.09)	0.01(0.00)	1.574(0.258)	0.742(0.031)	-	-
		Homo	0.94(0.10)	0.05(0.02)	2.972(0.046)	0.503(0.005)	-	-
		Proposed	0.90(0.06)	0.00(0.00)	0.437(0.198)	0.808(0.019)	2.0(0.0)	1.00(0.00)
80	200	Oracle	1.00(0.00)	0.00(0.00)	0.021(0.008)	0.827(0.014)	2.0(0.0)	1.00(0.00)
		Ind	0.65(0.07)	0.00(0.00)	1.150(0.207)	0.771(0.024)	-	-
		Homo	1.00(0.00)	0.02(0.02)	2.942(0.025)	0.499(0.005)	-	-
		Proposed	0.97(0.05)	0.00(0.00)	0.148(0.146)	0.822(0.016)	2.0(0.0)	1.00(0.00)
40	200	Oracle	1.00(0.00)	0.00(0.00)	0.035(0.018)	0.829(0.014)	2.0(0.0)	1.00(0.00)
		Ind	0.48(0.10)	0.00(0.00)	1.658(0.279)	0.737(0.029)	-	-
		Homo	0.97(0.08)	0.03(0.01)	2.951(0.033)	0.499(0.002)	-	-
		Proposed	0.87(0.07)	0.00(0.00)	0.554(0.187)	0.806(0.017)	2.0(0.0)	1.00(0.00)
80	200	Oracle	1.00(0.00)	0.00(0.00)	0.025(0.009)	0.822(0.019)	2.0(0.0)	1.00(0.00)
		Ind	0.52(0.10)	0.00(0.00)	1.521(0.277)	0.742(0.043)	-	-
		Homo	0.94(0.11)	0.01(0.01)	2.917(0.019)	0.497(0.004)	-	-
		Proposed	0.86(0.10)	0.00(0.00)	0.482(0.304)	0.803(0.031)	2.0(0.0)	1.00(0.00)

source. The response variable denotes bid status, with $y_i = 1$ for successful bids and $y_i = 0$ otherwise, resulting in an overall success rate of 4.83%. After applying feature engineering techniques such as one-hot encoding for categorical variables and log transformation or standardization for continuous variables, as well as feature interaction generation, we finally generate $p = 57$ predictors. These predictors provide valuable information on both borrowers and bids, significantly influencing investors' decisions and bid outcomes.

After applying the proposed method to this dataset via a logistic model, we identified three subgroups of provinces: the first subgroup includes Guangdong, Fujian, Hunan, Hebei, and Jiangxi (5 provinces); the second subgroup comprises Zhejiang, Shandong, Hubei,

Sichuan, Henan, Anhui, and Guangxi (7 provinces); and the third consists solely of Beijing (1 province). Table 2 presents the results of variable selection and coefficient estimates for these subgroups, revealing 13, 10, and 10 significant variables, respectively, with substantial overlap and consistent coefficient signs across all models, though their magnitudes vary. Key factors influencing successful fundraising include smaller bid amounts, which align with expectations, while higher annual interest rates decrease the likelihood of success. Previous studies show that elevated interest rates correlate with higher loan default rates, impacting investor decisions (Polena and Regner 2018). In addition, borrower characteristics play vital roles; older individuals and those with a credit history tend to have higher success rates. Financial indicators, such as income level and car ownership, also significantly affect fundraising outcomes. For comparison, we apply the Oracle method, which confirms these findings, underscoring the effectiveness of the proposed method.

To evaluate the predictive performance of the proposed method, we split the data into training and testing sets, using batches 1 to 10 for training and batches 11 to 13 for testing. Table 3 reports the test AUC values for various models across different provinces, along with their averages. The average test AUC for the proposed method is 0.947, compared to 0.952 for Oracle, 0.805 for Ind, and 0.921 for Homo. This suggests that the proposed method outperforms the alternatives and is comparable to the infeasible Oracle method. This trend is consistent across provinces, with the proposed method generally achieving higher AUC values than the alternatives. Additionally, Figure S7 of the supplementary material presents the corresponding trace plot, indicating that the proposed method consistently surpasses the Ind method and progressively approaches the performance of the Oracle method. In summary, these findings highlight the predictive capabilities of the proposed method in real-world applications.

6.2. Analysis of web log data

We apply the proposed method to analyze bank web log data to detect potential cyber-attacks by identifying abnormal requests directed at its portal websites. In general, users

Table 2 Analysis of financial platform data: the variable selection and estimation results for the proposed estimation.

Variable	Description	Subgroup 1	Subgroup 2	Subgroup 3
BidAmount	The amount of money for the fundraising bid	-0.348	-0.485	-0.620
APR	Annual interest rate	-0.287	-0.338	-0.330
Age	Age	0.310	0.307	0.574
LoanNumbers	The number of successful loans	0.278	0.358	0.435
RepaymentPeriod_2	Repayment period for the bid (6 to 12 months)	-0.331	-0.472	
RepaymentPeriod_3	Repayment period for the bid (12 to 18 months)	-0.885		
sex_2	Sex: female	-0.252	-0.771	-0.647
MaritalStatus_1	Marital status: spinsterhood	-0.229		-0.156
SuccessfulNum_1	The number of previous successful fundraising bids (equals 1)	2.157	1.773	2.173
SuccessfulNum_2	The number of previous successful fundraising bids (equals 2)	1.212	1.201	
SuccessfulNum_6	The number of previous successful fundraising bids (larger than or equals 6)	0.479		0.886
IncomeLevel_1	Monthly Income level (Below 2000 yuan)	-0.106		
IncomeLevel_3	Monthly Income level (Below 2002 yuan)	0.204		
hasCar_2	The car ownership of the borrower	0.115		
jobType_1	Job type of borrower (salaried)	-0.423	-0.265	-0.468

Table 3 Analysis of financial platform data: test AUC results for different provinces.

	Oracle	Ind	Homo	Proposed
Guangdong	0.966	0.954	0.932	0.961
Zhejiang	0.949	0.740	0.931	0.934
Shandong	0.962	0.850	0.939	0.954
Fujian	0.949	0.900	0.917	0.946
Hunan	0.933	0.890	0.878	0.943
Hubei	0.968	0.601	0.904	0.944
Sichuan	0.935	0.590	0.927	0.942
Henan	0.963	0.887	0.916	0.962
Beijing	0.932	0.911	0.906	0.909
Hebei	0.962	0.939	0.930	0.965
Anhui	0.963	0.661	0.931	0.962
Guangxi	0.948	0.798	0.934	0.934
Jiangxi	0.940	0.747	0.929	0.952
Average	0.952	0.805	0.921	0.947

interact with websites mainly through Hypertext Transfer Protocol (HTTP) requests, most of which are “normal” from legitimate users, while some are “abnormal”, indicating possible cyberattacks. The web logs contain parameters submitted as a series of key-value pairs, with sample logs available in Table S11 of the supplementary material. Traditional security products, like intrusion prevention systems (IPS) and web application firewalls (WAF), primarily use comparison-based approaches, which can struggle with unknown or sophisticated attacks, such as zero-day exploits. In contrast, our method extracts features from web logs to develop statistical models for more flexible, real-time cyberattack detection.

The dataset contains parts of the web logs from $K = 11$ websites (named as $url1$ – $url11$), collected over 16 days (August 29 to September 9, 2019), with varying log volumes. The total samples for the websites range from 1,150 to 3,368, and we analyze a binary response variable where $y_i = 1$ indicates abnormal requests and $y_i = 0$ indicates normal requests. The overall abnormal rate is 34.85%, with individual rates between 24.40% and 50.06%. We performed feature engineering to generate $p = 45$ numerical predictors from the web logs, including total request length (Plen), parameter (key-value pairs) counts (Pnum), the lengths of various parameters (Pl0–Pl19), and the descriptions about various parameter types (Pcnt_num, Pratio_num, Pt0_str, Pt0_num, and Pt1_not_na–Pt19_not_na).

Using the proposed method, we group the 11 websites into 5 subgroups of sizes 4, 3, 2, 1 and 1, with models involving 9, 6, 28, 6 and 7 variables, respectively, showing substantial overlaps. The detailed results of the variable selection and estimation are summarized in Table S13 of the supplementary material. In particular, variables Pl0–Pl2 (lengths of the first to fourth parameters in the request) are selected for more than 4 subgroups with positive signs, indicating that abnormal requests may contain redundant contents. Other frequently selected variables include Pcnt_num (the number of parameters with type “num”), Pt0_str (whether the type for the first parameter is “str”), Pt0_not_na (whether the type for the first parameter is not “na”), and others. These findings provide valuable insights on cyberattack patterns.

To evaluate performance, batches 1 to 12 serve as the training dataset, while batches 13 to 15 are for testing. The results show that the average test AUC for the proposed method is 0.866, compared to 0.872 for Oracle, 0.857 for Ind, and 0.851 for Homo, demonstrating that the proposed method outperforms other alternatives and is comparable to the Oracle method. Detailed test AUC results for different websites and trace plots for the average test AUC across batches are provided in Table S14 and Figure S8 of the supplementary material. Overall, these results further confirm the effectiveness of the proposed method in practical applications.

7. Discussion and Conclusions

This article presents a federated online method for high-dimensional heterogeneous multisource streaming data analysis. We address issues of homogeneity and heterogeneity among data sources using a subgroup assumption for modeling. Our proposed penalized renewable estimation and proximal gradient descent algorithm simultaneously estimates coefficients, identifies important variables, and recovers subgroup structure among data sources. It does not require raw data transmission across sources and only relies on the current batch raw data and summary statistics from previous batches for model updates. This intuitive approach has several well-desired theoretical properties and offers a unique modeling strategy compared to existing approaches.

Future research directions include incorporating prior information, such as network connections or tree structures between data sources, to enhance multisource modeling. Additionally, we currently assume synchronous data arrival; developing approaches for asynchronous scenarios, where updates occur at different times, poses further challenges. Finally, while our methodology focuses on Generalized Linear Models (GLMs), it could be adapted for other statistical models like the Cox model or finite-mixture models.

References

Beck A, Teboulle M (2009) A fast iterative shrinkage-thresholding algorithm for linear inverse problems. *SIAM Journal on Imaging Sciences* 2(1):183–202.

Boyd S, Parikh N, Chu E, Peleato B, Eckstein J, et al. (2011) Distributed optimization and statistical learning via the alternating direction method of multipliers. *Foundations and Trends® in Machine Learning* 3(1):1–122.

Chen Y, Zhang Q, Ma S, Fang K (2024) Heterogeneity-aware Clustered Distributed Learning for Multi-source Data Analysis. *Journal of Machine Learning Research* 25(211):1–60, ISSN 1533-7928.

Fallah A, Mokhtari A, Ozdaglar A (2020) Personalized Federated Learning with Theoretical Guarantees: A Model-Agnostic Meta-Learning Approach. *Advances in Neural Information Processing Systems*, volume 33, 3557–3568 (Curran Associates, Inc.).

Gomes HM, Read J, Bifet A, Barddal JP, Gama J (2019) Machine learning for streaming data: State of the art, challenges, and opportunities. *ACM SIGKDD Explorations Newsletter* 21(2):6–22, ISSN 1931-0145.

Hector EC, Luo L, Song PXK (2023) Parallel-and-stream accelerator for computationally fast supervised learning. *Computational Statistics & Data Analysis* 177:107587, ISSN 0167-9473.

Huang Y, Zhang Q, Zhang S, Huang J, Ma S (2017) Promoting similarity of sparsity structures in integrative analysis with penalization. *Journal of the American Statistical Association* 112(517):342–350, ISSN 0162-1459.

Li Q, Zhou Y, Liang Y, Varshney PK (2017) Convergence Analysis of Proximal Gradient with Momentum for Nonconvex Optimization. *Proceedings of the 34th International Conference on Machine Learning*, 2111–2119 (PMLR), ISSN 2640-3498.

Luo L, Han R, Lin Y, Huang J (2023) Online inference in high-dimensional generalized linear models with streaming data. *Electronic Journal of Statistics* 17(2):3443–3471, ISSN 1935-7524, 1935-7524.

Luo L, Li L (2022) Online two-way estimation and inference via linear mixed-effects models. *Statistics in Medicine* 41(25):5113–5133, ISSN 1097-0258.

Luo L, Song PXK (2020) Renewable estimation and incremental inference in generalized linear models with streaming data sets. *Journal of the Royal Statistical Society: Series B (Statistical Methodology)* 82(1):69–97, ISSN 1467-9868.

Ma S, Huang J (2017) A concave pairwise fusion approach to subgroup analysis. *Journal of the American Statistical Association* 112(517):410–423, ISSN 0162-1459, 1537-274X.

Ma X, Lin L, Gai Y (2022) A general framework of online updating variable selection for generalized linear models with streaming datasets. *Journal of Statistical Computation and Simulation* 93(3):325–340, ISSN 0094-9655.

Maity S, Sun Y, Banerjee M (2022) Meta-analysis of heterogeneous data: Integrative sparse regression in high-dimensions. *Journal of Machine Learning Research* 23(198):1–50, ISSN 1533-7928.

McMahan B, Moore E, Ramage D, Hampson S, y Arcas BA (2017) Communication-Efficient Learning of Deep Networks from Decentralized Data. *Proceedings of the 20th International Conference on Artificial Intelligence and Statistics*, 1273–1282 (PMLR), ISSN 2640-3498.

Pei J, Liu W, Li J, Wang L, Liu C (2024) A Review of Federated Learning Methods in Heterogeneous Scenarios. *IEEE Transactions on Consumer Electronics* 70(3):5983–5999, ISSN 1558-4127.

Polena M, Regner T (2018) Determinants of Borrowers' Default in P2P Lending under Consideration of the Loan Risk Class. *Games* 9(4):82, ISSN 2073-4336.

Qi H, Wang F, Wang H (2025) Privacy Protection and Statistical Efficiency Trade-Off for Federated Learning. *INFORMS Journal on Computing* ijoc.2024.0554, ISSN 1091-9856, 1526-5528.

Qiu Y, Chen Y, Fang K, Yu L, Fang K (2024) Fraud Detection by Integrating Multisource Heterogeneous Presence-Only Data. *INFORMS Journal on Computing* ISSN 1091-9856.

T Dinh C, Tran N, Nguyen J (2020) Personalized Federated Learning with Moreau Envelopes. *Advances in Neural Information Processing Systems*, volume 33, 21394–21405 (Curran Associates, Inc.).

Toulis P, Airoldi EM (2017) Asymptotic and finite-sample properties of estimators based on stochastic gradients. *The Annals of Statistics* 45(4):1694–1727, ISSN 0090-5364.

Wang P, Liu B, Guo W, Li Y, Ge S (2024) Towards Personalized Federated Learning via Comprehensive Knowledge Distillation. *2024 IEEE International Conference on Systems, Man, and Cybernetics (SMC)*, 3807–3812.

Wen J, Zhang Z, Lan Y, Cui Z, Cai J, Zhang W (2023) A survey on federated learning: Challenges and applications. *International Journal of Machine Learning and Cybernetics* 14(2):513–535, ISSN 1868-808X.

Xie J, Yan X, Jiang B, Kong L (2024) Statistical inference for smoothed quantile regression with streaming data. *Journal of Econometrics* 105924, ISSN 0304-4076.

Yan Y, Niu C, Ding Y, Zheng Z, Tang S, Li Q, Wu F, Lyu C, Feng Y, Chen G (2024) Federated Optimization Under Intermittent Client Availability. *INFORMS Journal on Computing* 36(1):185–202, ISSN 1091-9856, 1526-5528.

Zhang CH (2010) Nearly unbiased variable selection under minimax concave penalty. *The Annals of Statistics* 38(2):894–942, ISSN 0090-5364.